Composites: Part B 57 (2014) 210–218

Contents lists available at ScienceDirect

Composites: Part B

journal homepage: www.elsevier.com/locate/compositesb

Effects of carbon nanotube enrichment of epoxy resins on hybrid FRP–FR confinement of concrete

Theodoros C. Rousakis [a,*], Katerina B. Kouravelou [b], Theodoros K. Karachalios [b]

[a] Laboratory of Reinforced Concrete, Department of Civil Engineering, Democritus University of Thrace (DUTh), 67100 Xanthi, Greece
[b] Nanothinx S.A., Rion, Achaia 26504, Greece

ARTICLE INFO

Article history:
Received 30 May 2013
Received in revised form 6 August 2013
Accepted 20 September 2013
Available online 1 October 2013

Keywords:
A. Polymer–matrix composites (PMCs)
B. Strength
D. Mechanical testing
A. Hybrid
A. Carbon nanotubes

ABSTRACT

The present research study is focused on the tensile testing and mechanical characterization of three different epoxy resins, reinforced with different concentrations of Multi-Walled Carbon Nanotubes (MWCNTs). The resins are used in crack repair of concrete members as well as in FRP sheet wrapping. The CNT reinforced polymers (CNTRP) showed a remarkable enhancement of their tensile strength (2.25 times over the host matrix) and deformation at failure (3.27 times over the host matrix). The CNTRP with the highest viscosity were used in a structural application, to impregnate glass FRP sheets to confine concrete cylinders. Then the specimens were wrapped with non-impregnated polypropylene fiber ropes (PPFR). The comparative results between specimens confined by the hybrid system, including glass sheets impregnated with epoxy resin or with resin reinforced by CNTs (CNTRP), are discussed. The specimen with CNT reinforced polymer showed 7.5% higher bearing load of the concrete until failure of the glass sheet, over the column with non-reinforced polymer. The gradual, smooth failure of the glass fiber CNTRP jacket took place at higher load levels than GFRP. Moreover, it presented half temporary load loss after the fracture of the glass sheet than the GFRP strengthened column. Finally, it indicated an earlier stabilization and regaining of the bearing load (27% earlier in terms of axial strain).

1. Introduction

Several fiber reinforcements in micro-scale diameters, are extensively used in structural applications for the upgrading of reinforced concrete (rc) structures. Especially the use of carbon and glass fiber reinforcements, impregnated with suitable resins (Fiber Reinforced Polymers, FRP) are well-established and growing in structural repair and strengthening of existing rc structures [1–10].

Nowadays, carbon reinforcement in nano-scale in the form of tubes attracts the interest of researchers that deal with concrete technology. It has been shown that carbon nanotubes could enhance the mechanical properties of concrete when used as mass reinforcement, even in a small content. Additionally they could enable for the strain registration of the structural member by presenting piezoresistivity [11,12]. Research also focuses on the control of porosity in nano-level, to avoid bond disturbances between nanofibers and cement paste [13,14].

Extensive research conducted so far, shows clearly that the proper enrichment of resins with carbon nanotubes can enhance remarkably the resin's mechanical properties in terms of elastic modulus, tensile strength, performance at elevated temperatures, etc [15 among else]. Yet, no applications exist so far in the knowledge of the authors towards external FRP strengthening technology.

Recently, a hybrid strengthening technique for concrete columns was proposed [16], that combined FRP sheets and fiber rope (FR) materials. The technique utilized the unique advantages of the ultra high extension capacity (or low modulus of elasticity) materials. Vinylon or polypropylene materials present very low sensitivity to local damage of fibers because of handling and scratching. In the form of continuous ropes they can withstand successfully stress concentrations in edges of noncircular sections or because of crack evolution. Thus, they need no resin impregnation or binders in external confinement applications. The experimental results in concrete specimens confined by vinylon or polypropylene fiber ropes showed that they could provide exceptional strength and strain enhancement to concrete [17]. Remarkable concrete axial strains around 13% have been achieved. As already mentioned, polypropylene fiber ropes can be used in hybrid confining schemes as outer wrapping in already FRP confined columns. In the research by Rousakis [16] it has been shown that the polypropylene fiber rope can withstand the fracture of the glass FRP sheet (FRP exhibits lower extension capacity). The

* Corresponding author. Address: Department of Civil Engineering, Democritus University of Thrace, Vas. Sofias 12, 67100 Xanthi, Greece. Tel.: +30 2541079645; fax: +30 2541079638.
E-mail address: trousak@civil.duth.gr (T.C. Rousakis).

1359-8368/$ - see front matter © 2013 Elsevier Ltd. All rights reserved.
http://dx.doi.org/10.1016/j.compositesb.2013.09.044

temporary load drop upon fracture initiation of the FRP sheet was successfully stabilized by proper fiber rope design. Therefore, load regaining followed while the abrupt load capacity loss marked in FRP confined columns was eliminated. The concrete columns with the hybrid FRP–FR confinement presented further increased strain ductility and axial load capacity.

This paper presents the effects of the enrichment of three epoxy resins, of different specific weight, with Multi-Walled Carbon Nanotubes (MWCNTs). These resins have already been used extensively for the crack repair of concrete members or the impregnation of fiber sheets for the external strengthening of reinforced concrete members [1–9]. Firstly, the optimum concentration of high-purity MWCNTs in the resins was investigated. The study presents the tensile mechanical properties of the enriched epoxy resin specimens with different carbon nanotube concentrations. The upgraded carbon nanotube reinforced polymer (CNTRP) with the highest viscosity was used to impregnate glass FRP sheets that confine concrete cylinders. Subsequently, the specimens were wrapped with unbonded non-impregnated polypropylene fiber ropes (PPFR). The comparative results between specimens confined by the hybrid FRP–FR system, including glass sheets impregnated with epoxy resin or with resin reinforced by CNTs (CNTRP), are discussed.

2. CNTRP specimens preparation and tensile testing

2.1. Materials and mixtures processing

The investigation employed three epoxy resins of type J158, S2 and S2WV (commercial products of Sintecno S.A., Greece). Each resin was enriched with MWCNTs of 97% purity over catalyst. The MWCNTs were produced using the Catalytic Chemical Vapor Deposition (CCVD) method, known for its versatility for the large scale and low cost production of CNTs. According to the CCVD method, suitable carbon precursors resulting from the decomposition of hydrocarbons or alcohols at elevated temperatures, 600–1000 °C, interact with the catalyst particles in the CCVD reactor and result in the growth of CNTs on them. In this case, the reaction took place inside a quartz tube hot-wall reactor, embedded in a three-zone, split-tube cylinder furnace, and the temperature was controlled by a system of three controllers with Pt/Pt–Rh thermocouples. The catalyst, specially fabricated of metallic nanoparticles, supported on ceramic substrates, were developed by Nanothinx S.A., Greece [18]. All the operational parameters were optimized for the production of very high purity CNTs, 97% over catalyst, with minimal carbon impurities. The MWCNTs material was characterized by Scanning Electron Microscopy (SEM), Transmission Electron Microscopy (TEM), Raman Spectroscopy and Thermogravimetric Analysis (TGA).

Fig. 1a shows the Scanning Electron Microscopy (SEM) characterization image of the MCWNTs additives. Their diameter ranges from 15 to 35 nm and their length is higher than 10 μm. Fig. 1b presents the Transmission Electron Microscopy (TEM) characterization image of the wall structure of the MCWNTs. In this image the nanoscale dimension and the tubular form of the carbon nanomaterial is being verified, by the presence of the internal space between the walls of the nanotube. Moreover the existence of multiple, concentric graphene layers, constituting the walls of the CNT, are being shown, while the characterization of the material by more TEM images certifies that the number of the walls varies between 20 and 40. In Fig. 2a, the Thermogravimetric Analysis of the MWCNTs is presented. During this analysis, the sample was being heated in oxygen atmosphere from room temperature to 810 °C, with a heating rate of 5 °C/min. The CNTs were being burned between 580 °C and 640 °C, while the catalyst remains at the end

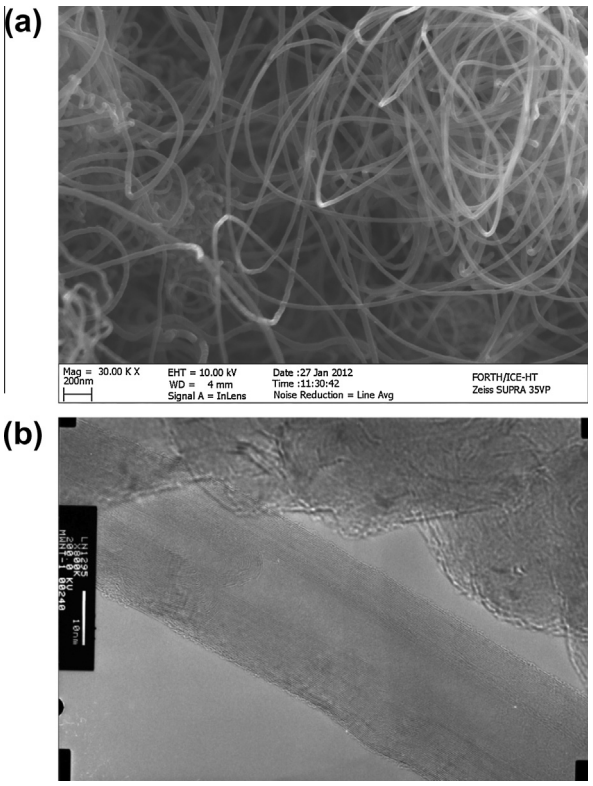

Fig. 1. Scanning Electron Microscopy image of the MWCNTs (a). Transmission Electron Microscopy image of the nanotube (b).

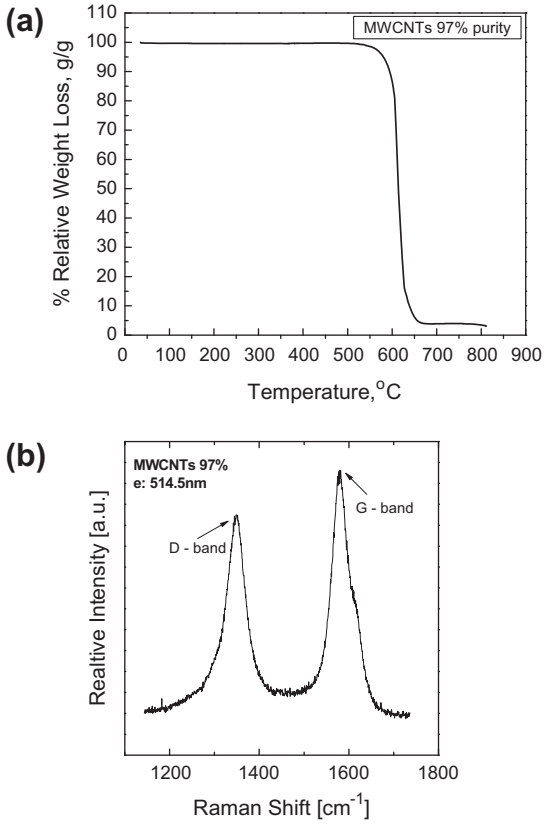

Fig. 2. Thermogravimetric Analysis of the MWCNTs (a). Raman Analysis of the MWCNTs (b).

Table 1
Experimental results.

	Density of resin (g/cm^3)	Content in MWCNT (%)	Modulus of elasticity E (GPa)	Maximum stress σ_m (MPa)	Strain at maximum stress ε_m (%o mm/mm)	Failure stress σ_u (MPa)	Failure strain ε_u (%o mm/mm)	Normalized maximum stress σ_m/σ_o	Normalized failure stress σ_u/σ_o	Normalized maximum strain $\varepsilon_m/\varepsilon_o$	Normalized failure strain $\varepsilon_u/\varepsilon_o$
J158	0.9	0	3.2	31.75	9.77	31.75	9.77				
J158_0.25%#1	0.9	0.25	3.5	69.3	25.1	69.3	25.1	2.18	2.18	2.57	2.57
J158_0.25%#2	0.9	0.25	3.5	71.48	26.07	71.48	26.07	2.25	2.25	2.67	2.67
J158_0.25% (average)	0.9	0.25	3.5	70.39	25.585	70.39	25.585	2.22	2.22	2.62	2.62
J158_0.5%#1	0.9	0.5	3.1	53.82	18.5	53.82	18.5	1.70	1.70	1.89	1.89
J158_0.5%#2	0.9	0.5	3.4	59.47	19.65	59.47	19.65	1.87	1.87	2.01	2.01
J158_0.5% (average)	0.9	0.5	3.25	56.645	19.075	56.645	19.075	1.78	1.78	1.95	1.95
S2#1	1.1	0	1.8	28.77	17.03	28.77	17.03				
S2#2	1.1	0	1.8	21.11	13.11	21.11	13.11				
S2 (average)	1.1	0	1.8	24.94	15.07	24.94	15.07				
S2_0.25%#1	1.1	0.25	1.75	40.22	32.16	40.22	32.16	1.61	1.61	2.13	2.13
S2_0.25%#2	1.1	0.25	1.75	43.73	43.82	43.73	43.82	1.75	1.75	2.91	2.91
S2_0.25% (average)	1.1	0.25	1.75	41.975	37.99	41.975	37.99	1.68	1.68	2.52	2.52
S2_1%#1	1.1	1	1.5	23.8	21.26	23.8	21.26	0.95	0.95	1.41	1.41
S2WV#1	1.15	0	2.2	35.65	37.09	32.9	63.5				
S2WV#2	1.15	0	2.2	33.95	47.44	31.53	71.08				
S2WV (average)	1.15	0	2.2	34.8	42.265	32.215	67.29				
S2WV_0.125%#1	1.15	0.125	2.2	32.83	42.54	30.25	92.78	0.94	0.87	1.01	2.20
S2WV_0.125%#2	1.15	0.125	2.2	30.53	50.43	28.15	138	0.88	0.81	1.19	3.27
S2WV_0.125% (average)	1.15	0.125	2.2	31.68	46.485	29.2	115.39	0.91	0.84	1.10	2.73
S2WV_0.25%#1	1.15	0.25	2.1	31.78	42.37	30.15	76.65	0.91	0.87	1.00	1.81
S2WV_0.25%#2	1.15	0.25	2.2	30.8	43.43	29.42	108	0.89	0.85	1.03	2.56
S2WV_0.25% (average)	1.15	0.25	2.15	31.29	42.9	29.785	92.325	0.90	0.86	1.02	2.18

J158, S2, S2WV: type of resin of different viscosity. Low viscosity J158 injective resin for use in capillary concrete cracks, S2 injective resin for use in concrete cracks, of S2WV resin for use in fiber sheet impregnation.
0.125%, 0.25%, 0.5%: wt. concentrations of MWCNTs used to enrich the resins.
#1, #2: number of identical specimens.

of the procedure. By this analysis it was deduced that the remaining catalyst was only 3% of the initial sample, while no other carbon impurities, like amorphous carbon (that was being burned between 360 °C and 400 °C), were present in the MWCNTs used. For the Raman characterization of the MWCNTs material, a laser excitation of wavelength 514.5 nm was used, and the laser's power focused in the sample was 1.93 mW. In Fig. 2b, the spectrum in the frequency range of, approximately, 1200–1800 cm^{-1} is being presented. The two characteristic peaks of the MWCNTs, namely the D-band and the G-band, are presented. The G-band, is characteristic of the sp^2 hybridization of the graphite, is stronger and appears in the range of 1570–1590 cm^{-1}. The D-band, is weaker than the G-band, appears at about 1350 cm^{-1}, and is being attributed to the defects of the graphene layer or the CNT due to the curvature of the tube and the closing of the graphene sheet [19].

The MCWNTs additives were mixed with the resins in different carbon nanotubes concentrations that varied between 0 and 1 wt.% (Table 1) to form dogbone specimens for tensile tests, with their characteristics (based on ASTM D638) shown in Fig. 3. The specimens preparation procedure included mechanical mixing of the MWCNTs in the epoxy resins and mild sonication of the composite resin, at 140W for a few minutes (instrument Hielscher UP400S), in order to improve the dispersion of CNTs in the resin. Afterwards, the appropriate hardener of the epoxy resin was added and the mixture was cast in the corresponding dogbone mold, and let to cure at room temperature.

In Figs. 4–6, the SEM images of the dispersions of CNTs in the J158, S2 and S2WV resins are presented respectively. CNTs are depicted as white spots inside the resin matrix, which is represented by the dark area in the SEM images. In some images the CNTs come out from the epoxy matrix and are shown as white lines. The accumulation of white areas in the SEM images is evident of the existence of CNTs aggregates.

The resin of type J158 had the lowest viscosity and is suitable for use as injective resin in capillary cracks. Different concentrations of MWCNTs were investigated in order to achieve the optimum dispersion. Fig. 4 shows the SEM characterizations of the J158 specimens enhanced with three different MWCNTs concentrations. As noticed in Fig. 4a, the dispersion of 0.25 wt.% of MWCNTs inside J158 resin, is efficiently good. For 0.35 wt.% concentration, Fig. 4b, the dispersion is acceptably good, however there is a tendency of CNTs agglomeration, which is evident in higher concentrations, such as 0.5 wt.% in Fig. 4c, where CNTs aggregates are shown in the picture.

Similarly, the dispersions of MWCNTs in the S2 resin are presented, for three concentrations 0.25%, 1% and 2.5% wt., in Fig. 5. The efficient dispersion of MWCNTs in S2 is proved to be a more difficult task, due to the higher viscosity of this resin. Nevertheless, for very low concentrations, up to 0.25 wt.% shown in Fig. 5a, the dispersion can be acceptable for the enhancement of the resin's mechanical properties. However, for higher concentrations, 1 wt.% shown in Fig. 5b and 2.5 wt.% shown in Fig. 5c, the presence of great CNTs agglomerates are expected to affect negatively the enhancement of the mechanical properties of composite resin.

For the resin of type S2WV, which has similar viscosity with S2, two low concentrations of MWCNTs were examined, namely 0.125 wt.% and 0.25 wt.% shown in Fig. 6, in order to avoid great CNTs agglomerations. The dispersion in both concentration was satisfactory, with negligible areas of CNTs aggregates, mainly observed in the higher concentration. Finally, it should be pointed out that non-homogeneous dispersion was, also, observed in multi-walled carbon nanotube reinforced polymers (CNTRPs) with

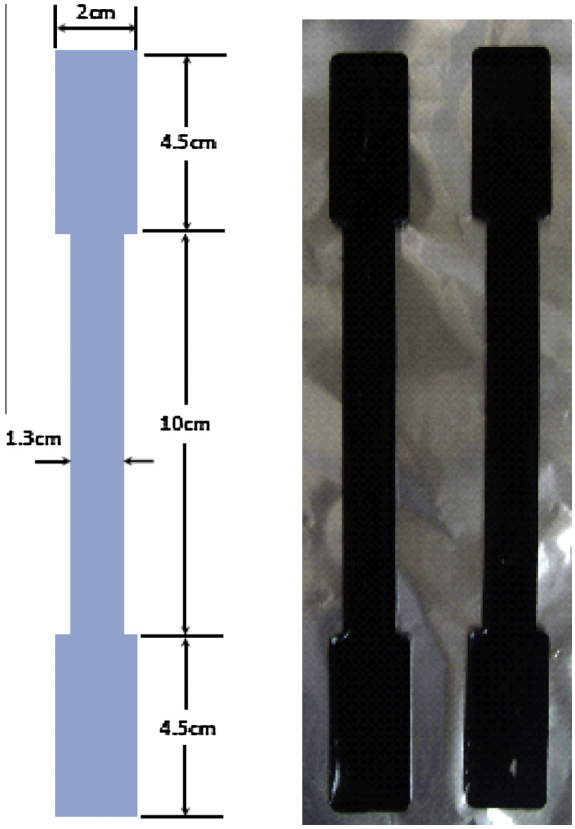

Fig. 3. Detailing of dogbone specimens and characteristic view of the specimens of J158_0.5% series.

very low CNTs concentrations, less than 0.1 wt.%, due to the insufficient quantity of CNTs in the resin.

2.2. Tensile testing of CNTRPs

Standard dogbone specimens of CNTRPs were tested under direct tension to acquire their mechanical behavior. The results of the average of two identical specimens per different resin with different MWCNTs concentration are gathered in Table 1. The tests have been executed in a servo hydraulic tensile machine of MTS type with 250 KN capacity. Due to the high strain achieved, a special laser displacement meter was used to measure the deformation of the specimens between attached targets.

Fig. 7a presents the test setup of the tensile testing and the obvious necking of the CNTRP S2WV_0.125% during loading. The necking was typical for MWCNTs enriched resins, as observed also in Fig. 7c for CNTRP J158_0.25%. On the other hand, Fig. 7b shows a typical failure for resin J158 without obvious residual deformations and thus no local necking.

The stress–strain curves of the tested specimens are included in Figs. 8–10. Fig. 11 presents a comparative diagram for all three series of different composites. S2WV specimens showed a plastic-like behavior and high deformation at failure (Fig. 10). Herein, it is reminded that a clear neck was formed in the S2WV polymers reinforced with CNTs (Fig. 7a). A less pronounced neck-like shape formed also in J158 reinforced polymers that corresponds to the elastic-like stress–strain behavior (Fig. 7c).

The low viscosity resin J158 with only 0.25 wt.% MWCNTs, presented more than twofold stress and strain upgrade at failure with upgraded behavior. FRP impregnation resin S2WV with 0.125 wt.% MWCNTs exhibited 2.73 times higher failure strain than plain S2WV (in average values) and a plastic-like behavior.

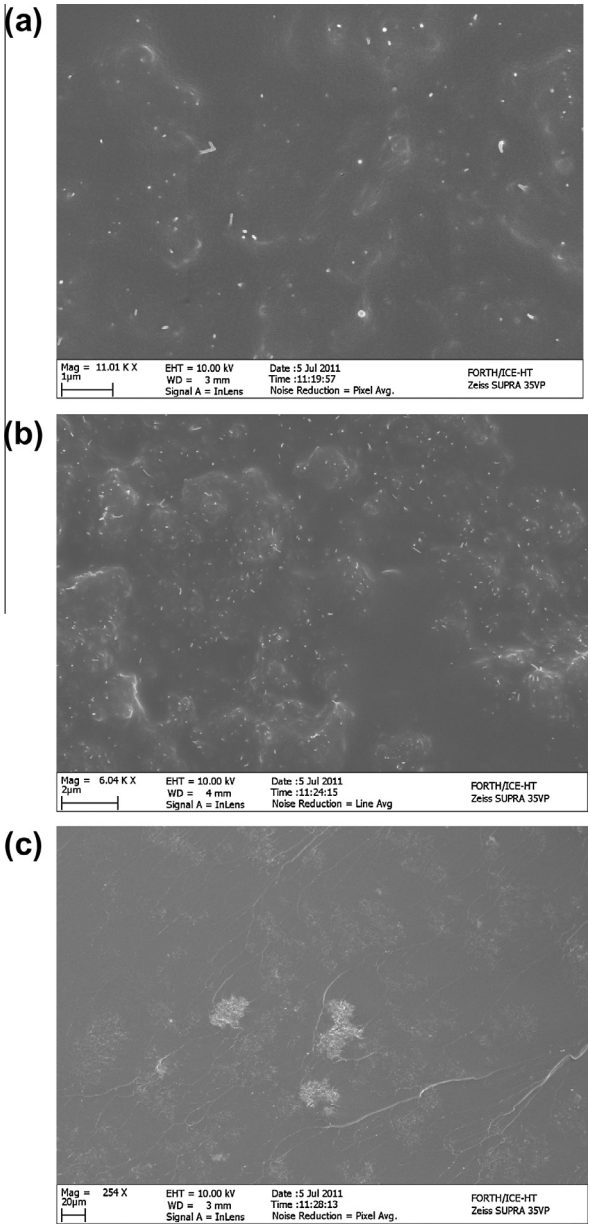

Fig. 4. Scanning Electron Microscopy images of the J158 resin (a) enhanced with 0.25 wt.% MWCNTs, (b) enhanced with 0.35 wt.% and (c) enhanced with 0.5 wt.% MWCNTs.

It seems that the effect on stress transfer was lower in high viscosity resins. However this is observed for lower CNTs concentrations (0.125 wt.% for high viscosity resins, compared to the 0.25 wt.% for the low viscosity J158 resin), were the optimum dispersion was achieved.

The samples with MWCNTs concentrations of the optimum dispersion, as observed in the SEM images, in terms of mixture homogeneity, provided the highest upgrade of the mechanical behavior regarding failure load and deformation.

The CNTRP S2WV_0.125% reached an average tensile failure strain of 11.5%. This deformability performance of the enhanced matrix, could ensure the continuous load transfer among resin-impregnated reinforcing fibers of high extension capacity (vinylon, PET, PEN, polypropylene, etc). The J158_0.25% and S2 CNTs enriched resins could be used for the crack repair of high performance or very high strength concrete. However, they could not be used as impregnating resins for hand lay-up application of

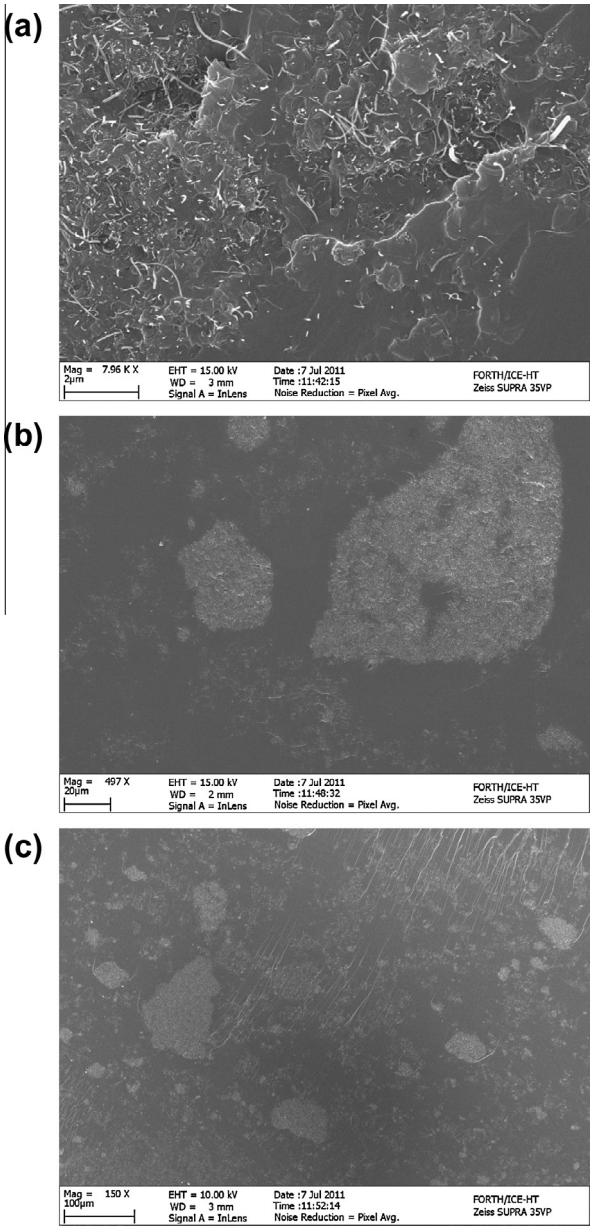

Fig. 5. Scanning Electron Microscopy images of the S2 resin (a) enhanced with 0.25 wt.% MWCNTs, (b) enhanced with 1 wt.% and (c) enhanced with 5.5 wt.% MWCNTs.

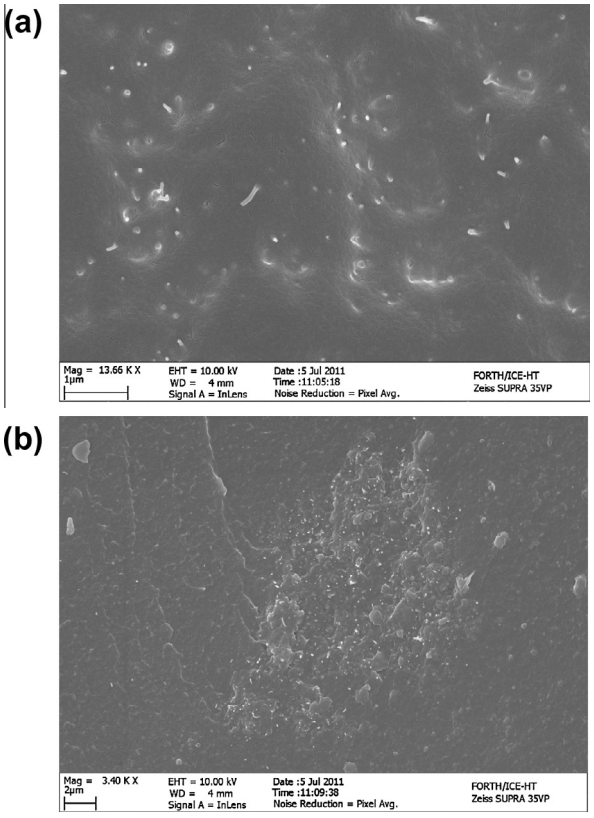

Fig. 6. Scanning Electron Microscopy images of the S2WV resin (a) enhanced with 0.125 wt.% MWCNTs, and (b) enhanced with 0.25 wt.% MWCNTs.

FRP sheets because of their low viscosity. All resins could be used for the production of enhanced FRP laminates for external strengthening.

3. GF–CNTRP–PPFR concrete specimens preparation and compression testing

3.1. Materials, strengthening scheme and test setup

The enhanced nano-reinforced polymers were tested in confinement strengthening of standard concrete cylinders to impregnate E-glass sheets. The MWCNTs reinforced resin S2WV_0.125% was used, since it exhibited the highest strain at failure, equal to 11.5% (average of two specimens).

The results presented in this study are part of an extended investigation of different confinement techniques using FRP or PPFR or a combination of them, for a range of different concrete strengths [16]. Herein, three externally strengthened columns are compared that belong to C16 batch of concrete cylinders with 150 mm diameter and 300 mm height. The batch had 25.1 MPa average concrete strength during the tests. The glass fiber sheet was a S&P G90/10 type unidirectional sheet with 300 mm width, impregnated by S2WV resin (S&P—Sintecno, [20]). The structural thickness of the FRP was 0.154 mm, the tensile modulus of elasticity 73 GPa and the strain at failure 2.8%. The polypropylene fiber rope (PPFR, product of Thrace Plastics Co. S.A., see Fig. 12b) was a Z-twisted two-strand one with 11 g/m, a tensile modulus of elasticity of only 2.0 GPa and 20.36% elongation at failure.

Two columns were confined by one layer of glass sheet. The first one was impregnated by S2WV_0.125% CNTRP (Fig. 12a) while the second one was impregnated by plain S2WV resin for comparison. After the curing of the polymers, both columns were additionally confined by three layers of high deformability non-impregnated PPFR. The third column presented here was confined only by five layers of PPFR.

The columns were imposed to concentric repeated axial compression–decompression–recompression cycles, with manual deformation control. The initial cycles had a step of around 0.05% compressive strain in order to capture the unique temporary load drop that was evidenced in PPFR confined concrete cylinders. After the point of load regaining, the step was increased gradually to more than 1% strain. The same mode of loading was followed for specimens with hybrid confinement. The strain recordings presented in this paper were provided by a variable displacement transducer (LVDT) that measured the displacement between the loading platens of the compression machine.

Previous studies have pointed out that PPFR confinement could maintain the integrity of concrete up to extraordinary levels of

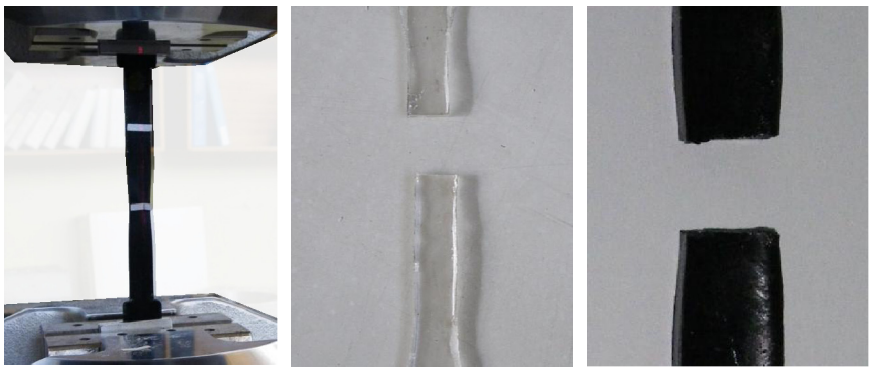

(a) Tensile testing scheme. Necking in CNTRP S2WV_0.125%

(b) CNTRP J158 after failure

(c) Necking in CNTRP J158_0.25% after failure.

Fig. 7. Testing scheme and typical failures of different CNTRP specimens.

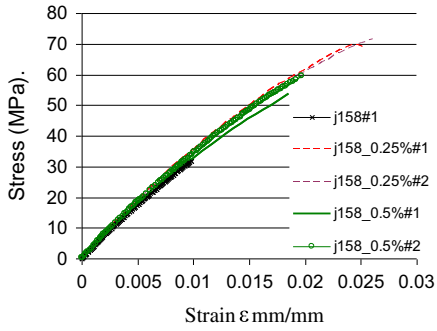

Fig. 8. Mechanical behavior of J158 resin samples reinforced by CNTs under direct tension.

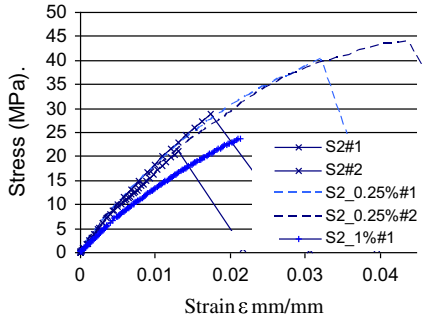

Fig. 9. Mechanical behavior of S2 resin samples reinforced by CNTs under direct tension.

compressive axial strain ductility [17]. The PPFR presented very low sensitivity to local concrete cracking and could easily redistribute the confining action throughout loading. When used in a hybrid scheme with glass FRP jacket, PPFR outer confinement could withstand the energy released by the fracture of the GFRP (it has lower deformability and thus it fractured first). The failure of the GFRP became gradual and in multiple regions of the jacket all over the cylinder perimeter due to the friction between GFRP and PPFR wrap [16]. After a temporary load drop the PPFR took over, leading to further increased load and strain ductility. The explosive glass FRP fracture was avoided and no PPFR fracture occurred for axial strain higher than 5%. This unique advantage of the PPFR confinement is utilized herein. As mentioned above, the PPFR was applied by hand and without resin impregnation. It was anchored in both ends (top and bottom) by the use of thin steel collars.

3.2. Compression testing of GF–CNTRP–PPFR confined concrete

This section discusses the comparative results of the behavior of the concrete column with external strengthening by five layers of PPFR or by one layer of GFRP and three layers of PPFR or by one layer of glass fiber CNTRP (GF–CNTRP) and three layers of PPFR in order to assess the MWCNTs effects.

In Fig. 12b it is observed that the PPFR confinement prevented the explosive failure of concrete at the point of the fracture of glass sheet in all cases. Also, it maintained the bearing load at high levels. It should be mentioned that both GFRP–PPFR and GF–CNTRP–PPFR specimens did not fail. Given the performance of external PPFR confinement in previous studies, the testing was terminated upon stabilization of the load at a lower level and initiation of load regaining at a high level of strain.

Fig. 13 denotes that the column, confined by five layers of PPFR, reached the stress of 27.6 MPa at 0.4% strain and then it presented a temporary load drop of only 1.58 MPa. The column had already reached 34 MPa stress at 3% axial strain and could maintain an increased load-bearing capacity for strain far higher than 6% without fiber rope fracture. The test was early terminated because of the unsafe steel collar's dislocation. The specimen is comparable with the hybrid ones in terms of confinement lateral rigidity PPFR possesses 87% of the corresponding lateral rigidity of the hybrid specimens provided by both FRP and FR.

The experimental mechanical stress–strain behavior of specimens with hybrid confinement is also depicted in Fig. 13. The column with hybrid FRP–FR confinement presented a typical FRP confined concrete behavior up to the initiation of FRP jacket fracture (at 40.4 MPa stress and 1.635% strain). Then a temporary and smooth load drop of 6.5 MPa happened (16.1%). The restriction provided by the PPFR and the interaction with the fractured FRP jacket managed to control the explosive fracture of the FRP and succeeded a stress of 34 MPa at 3% axial strain. This stress is identical to the one of PPFR confined column at 3% strain. The hybrid column presented far higher load values up to FRP fracture and to 3% strain but a lower bearing load afterwards. Also, it demonstrated a lower rate of load increase after 3% since the FRP jacket had already fractured. The FRP jacket corresponded to 44% of the total provided lateral rigidity.

The concrete specimen with only 0.125 wt.% MWCNTs in the S2WV impregnation resin, exhibited enhanced behavior compared to the counterpart of the common GFRP system with PPFR. The

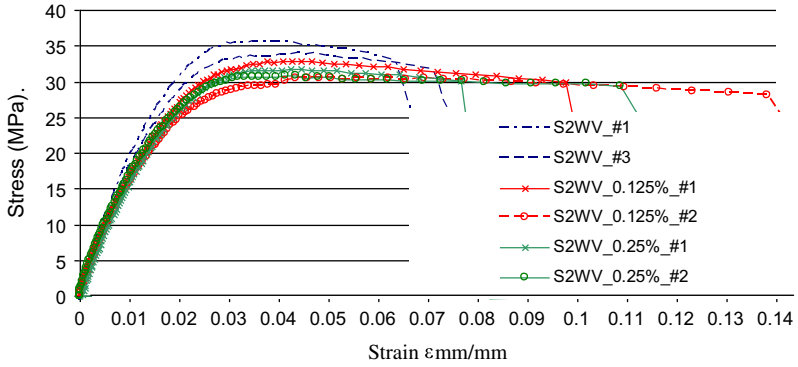

Fig. 10. Mechanical behavior of S2WV resin samples reinforced by CNTs under direct tension.

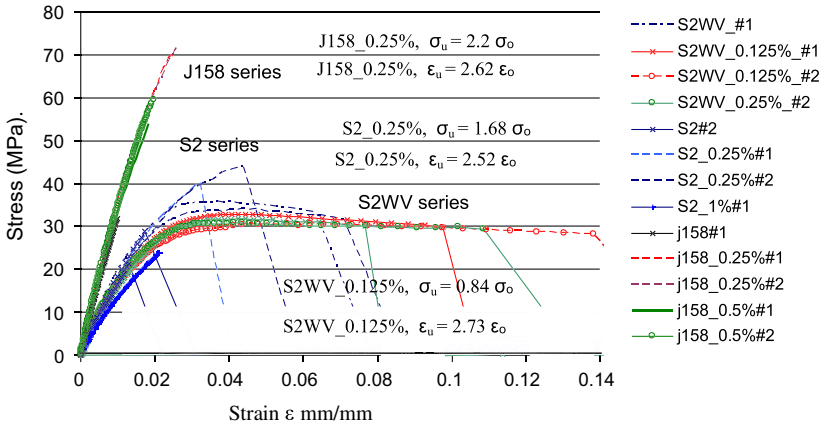

Fig. 11. Comparative diagram of the mechanical behavior of different resins reinforced by CNTs under direct tension.

(a) Concrete cylinder after wrapping with GF-CNTRP (polymer S2WV_0.125%)

(b) Hybrid confined GF-CNTRP-PPR concrete cylinder after failure

Fig. 12. Hybrid confined concrete specimens.

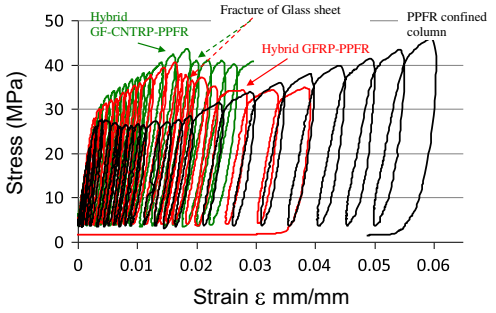

Fig. 13. Mechanical behavior of concrete standard cylinders confined by hybrid confining reinforcements.

maximum stress of the GR–CNTRP–PPFR strengthened column was 43.45 MPa which was 7.5% higher than that of the identical column impregnated with the S2WV resin (without MWCNTs enrichment). The maximum stress happened at a strain of 1.858% which was higher, correspondingly. The GF–CNTRP reinforcement fractured gradually and the bottom stress during the temporary load drop phase, was 39.65 MPa. This recording revealed a 8.7% load loss which was almost half of the corresponding for the specimen without MWCNTs (16.1%). Finally, the load regaining came at a strain of 2.666% which was 27% earlier than the column without MWCNTs enhancement (load regaining at 3.66% strain). Its overall behavior, in terms of bearing load, was also better than the one of the column with PPFR with almost equivalent lateral rigidity of the confinement.

The high levels of axial strain of concrete achieved herein, should be further elaborated for design purposes, as different types of failure may limit the usable axial strain value. Limit values of lateral and axial strains are adopted by design recommendations [21,22] and should be taken into account. Also, member instability issues may become critical because of the decrease of the modulus in the stress–strain curve after the extensive cracking of concrete and especially after the fracture of the FRP sheet [23–25,4].

4. Conclusions

The use of MWCNTs in repair and strengthening epoxy resin systems for rc members was investigated. The mechanical properties of the epoxy resins were remarkably enhanced even with a small content of nanotubes. Microscopically observed CNTs optimum dispersion, agreed well with the cases of the highest mechanical upgrade of resins, which was more than twofold in strength and deformation capacity for the present investigation. The lower the density or the viscosity of the resin, the higher the optimum amount of dispersed CNTs in the resin, and the higher the effect on tensile strength.

MWCNTs enriched resins presented necking around the mid-height of the specimens during tensile loading. Residual deformations were evident after the fracture of the specimens.

Impregnation of the glass sheet reinforcement by the advanced CNTRP resulted in upgraded behavior of the confined concrete when compared with the GFRP confined counterpart. The GF–CNTRP–PPFR confined column presented 7.5% higher maximum stress at higher axial strain, lower temporary load loss after glass jacket fracture and earlier load regaining (27% lower axial strain at load regaining). Of course more experimental tests are required to address the enhancement of the mechanical properties of the CNTRP impregnated glass sheets. Then, analytical modeling of the effects of the use of CNTs in confinement could be possible. Tensile test results revealed also a potential of the CNTs reinforced polymers for use in advanced crack repair of high performance concrete or in production of precured FRP laminates, as the viscosity of the resins was not reduced remarkably by the addition of MWCNTs.

Acknowledgements

Authors would like to thank Sintecno S.A. for providing the resins and the glass FRP sheets (S&P), Zaras S.A. for providing concrete and Thrace Plastics Co., S.A. for providing PP ropes. Also, thanks are owed to Dr. Vassilis Drakopoulos, Principal Scientist at FORTH/ICE-HT, for his assistance with the SEM analysis, Dr. Amaia Soto Beobibe, for her assistance with Raman characterization as well as to Sophias C., Metaxa Z., Tsakiris S. (help in tensile tests, with Metal Structures, Mechanics Labs equipment), Gouma M. and Anezakis M. (compression tests) for their help in execution of some of the tests and to DUTh RC lab staff.

References

[1] De Lorenzis L, Tepfers R. Comparative study of models on confinement of concrete cylinders with fiber-reinforced polymer composites. ASCE J Compos Constr 2003;7(3):219–34.
[2] Karantzikis M, Papanicolaou CG, Antonopoulos CP, Triantafillou TC. Experimental investigation of nonconventional confinement for concrete using FRP. J Compos Constr 2005;9(6):480–7.
[3] Tamuzs V, Tepfers R, You Chi-Sang, Rousakis T, Repelis I, Skruls V, et al. Behavior of concrete cylinders confined by carbon-composite tapes and prestressed yarns 1. Experimental data. Mech Compos Mater 2006;42(1):13–32.
[4] Valdmanis V, De Lorenzis L, Rousakis T, Tepfers R. Behavior and capacity of CFRP-confined concrete cylinders subjected to monotonic and cyclic axial compressive load. Structural concrete. J Fib 2007;8(4).
[5] Barros JAO, Ferreira DRSM. Assessing the efficiency of CFRP discrete confinement systems for concrete cylinders. J Compos Constr 2008;12(2):134–48.
[6] Rousakis TC, Karabinis AI, Kiousis PD. FRP-confined concrete members: axial compression experiments and plasticity modelling. Eng Struct J 2007;29(7):1343–53.
[7] Rousakis TC, Karabinis AI, Kiousis PD, Tepfers R. Analytical modelling of plastic behaviour of uniformly FRP confined concrete members. J Compos Part B: Eng 2008;39(7–8):1104–13.
[8] De Luca A, Nardone F, Matta F, Nanni A, Lignola G, Prota A. Structural evaluation of full-scale FRP-confined reinforced concrete columns. J Compos Constr 2011;15(1):112–23.
[9] Jian-Guo Dai, Yu-Lei Bai, Teng JG. Behavior and modeling of concrete confined with FRP composites of large deformability. J Compos Constr 2011;15(6):963–73.
[10] Wie Y, Wu Y. Unified stress–strain model of concrete for FRP-confined columns. Constr Build Mater 2012;26(1):381–92.
[11] Li GY, Wang PM, Zhao X. Pressure-sensitive properties and microstructure of carbon nanotube reinforced cement composites. Cem Concr Compos 2007;29(5):377–82.
[12] Azhari F, Banthia N. Cement-based sensors with carbon fibers and carbon nanotubes for piezoresistive sensing. Cem Concr Compos 2012;34(7):866–73.
[13] Sobolev K, Ferrada-Gutiérrez M. How nanotechnology can change the concrete world. Part 1. Am Ceram Soc Bull 2005;84(10):14–7. http://www.nano-tsunami.com.
[14] Tepfers R. Investigation of different types of fibers to strengthen cement paste, mortar and concrete. Department of Civil and Environmental Engineering Structural Engineering, Concrete Structures Report No. 2008:7 Chalmers University of Technology, SE-412 96 Göteborg, Sweden; 2008.
[15] Eitan A, Fisher FT, Andrews R, Brinson LC, Schadler LS. Reinforcement mechanisms in MWCNT-filled polycarbonate. Compos Sci Technol 2006;66:1162–73.
[16] Rousakis T. Hybrid confinement of concrete by FRP sheets and fiber ropes under cyclic axial compressive loading. J Compos Constr 2013;17(5):732–43.
[17] Rousakis TC. Elastic fiber ropes of ultra high extension capacity in strengthening of concrete through confinement. J Mater Civil Eng 2013. http://dx.doi.org/10.1061/(ASCE)MT.1943-5533.0000796.
[18] Nitodas SF, Karachalios TK. Low-cost production and applications of high purity carbon nanotubes. Int J Nanomanuf 2010;6(1/2/3/4):111–24.
[19] Eklund PC, Holden JM, Jishi RA. Vibrational modes of carbon nanotubes; Spectroscopy and theory. Carbon 1995;33(7):959–72.
[20] Scherer J. S&P-Sintecno, FRP-polymer fibers in strengthening. User guide. Brunnen; 1999.
[21] American Concrete Institute, Guide for the design and construction of externally bonded FRP systems for strengthening concrete structures. ACI 440.2R-08, Detroit; 2008.

[22] CNR-DT 200/2004. Guide for the design and construction of externally bonded FRP systems for strengthening existing structures. National Research Council, Advisory committee on technical recommendations for construction, Rome July 13th; 2004.
[23] De Lorenzis L., Tamužs V., Tepfers R., Valdmanis V., Vilks U. Stability of CFRP confined columns. IMTCR 2004. In: Innovative materials and technologies for construction and restoration conference, Lecce, June 6–9; 2004. pp. 327–42.
[24] Jiang T, Teng JG. Behavior and design of slender FRP-confined circular RC columns. ASCE, J Compos Constr 2012. http://dx.doi.org/10.1061/(ASCE)CC.1943-5614.0000333.
[25] Tamužs V, Valdmanis V, Tepfers R, Gylltoft K. Stability analysis of CFRP-wrapped columns strengthened with external longitudinal CFRP sheets. Mech Compos Mater 2008;44(3):199–208.